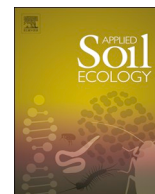




ELSEVIER

Contents lists available at ScienceDirect

## Applied Soil Ecology

journal homepage: [www.elsevier.com/locate/apsoil](http://www.elsevier.com/locate/apsoil)

# Temperature and water-level effects on greenhouse gas fluxes from black ash (*Fraxinus nigra*) wetland soils in the Upper Great Lakes region, USA

Alan J.Z. Toczydlowski<sup>a,\*</sup>, Robert A. Slesak<sup>a,b</sup>, Randall K. Kolka<sup>c</sup>, Rodney T. Venterea<sup>d</sup>

<sup>a</sup> Department of Forest Resources, University of Minnesota, 1530 Cleveland Ave N, St Paul, MN 55108, USA

<sup>b</sup> Minnesota Forest Resources Council, 1530 Cleveland Ave N, St Paul, MN 55108, USA

<sup>c</sup> USDA Forest Service, Northern Research Station, 1831 Hwy. 169 E, Grand Rapids, MN 55744, USA

<sup>d</sup> USDA-ARS, Soil and Water Management Unit, 1991 Upper Buford Cir, St Paul, MN 55108, USA

## ARTICLE INFO

## Keywords:

Greenhouse gas fluxes  
Methane  
Nitrous oxide  
Emerald ash borer  
Forested wetlands  
Soil core incubation  
Soil redox

## ABSTRACT

Forested black ash (*Fraxinus nigra*) wetlands are an important economic, cultural, and ecological resource in the northern Great Lake States, USA, and are threatened by the invasive insect, emerald ash borer (*Agrilus planipennis* Fairmaire [EAB]). These wetlands are likely to experience higher water tables and warmer temperatures if they are impacted by large-scale ash mortality and other global change factors. Therefore, it is critical to understand how temperature, hydrology, and their interaction affect greenhouse gas fluxes in black ash wetland soils. In order to predict potential ecosystem changes, we sampled and incubated intact soil cores containing either mineral or organic (peat) soils from two black ash wetlands, monitored soil oxidation-reduction potential (Eh), and measured the efflux of carbon dioxide (CO<sub>2</sub>), methane (CH<sub>4</sub>), and nitrous oxide (N<sub>2</sub>O) at two water-level treatments nested in three temperature treatments, 10 °C, 15 °C, or 20 °C. The water-level treatments were either saturated or drawdown, designed to mimic wetlands impacted or not impacted by EAB. Mean CO<sub>2</sub> fluxes increased with increasing temperature but did not vary significantly by soil type or water-level. Peat soil had 60 to 135 times significantly greater CH<sub>4</sub> flux in the saturated treatment and had minimal N<sub>2</sub>O loss across all treatments, while mineral soils had 8 to 43 times significantly greater N<sub>2</sub>O flux in the saturated treatment, and minimal CH<sub>4</sub> loss across all treatments. Gas fluxes generally increased and had greater variation with increasing temperature. The drawdown treatment resulted in significantly higher Eh during unsaturated periods in both soil types, but the response was more variable in the peat soil. Our findings demonstrate potential indirect effects of EAB in black ash wetlands, with implications for ecosystem functions associated with C and N cycling.

## 1. Introduction

In the northern Great Lakes region (Upper Michigan, Wisconsin, and northern Minnesota), many forests have significant components of ash (*Fraxinus* spp.) in the overstory, which are especially vulnerable to changes in composition and succession sequences following emerald ash borer (EAB) infestation (MacFarlane and Meyer, 2005). Since its discovery in the United States in 2002, EAB has spread quickly across the country, killing ash forests within 6 years of infestation (Herms and McCullough, 2014; Knight et al., 2013; Smitley et al., 2008). The invasion of EAB and large-scale ash dieback can decrease litter input, increase amounts of large woody debris, and cause canopy gap formation; cascading effects that may lead to large-scale changes in ecosystem structure, food web interactions, and altered biogeochemical cycling (Kolka et al., 2018). Forested black ash (*F. nigra*) wetlands are

especially prone to ecosystem-scale changes because ash makes up 40–100% of the canopy (Looney et al., 2015; Van Grinsven et al., 2017), they are already experiencing ash dieback (Palik et al., 2012, 2011), and transpiration by ash trees is a major control on hydrology (Telander et al., 2015). Ash mortality in these ecosystems causes the water table to rise, potentially transitioning a forested ecosystem to an open marsh (Slesak et al., 2014; Diamond et al., 2018). This groundwater sensitivity to transpiration makes forested ash wetlands especially vulnerable to altered ecosystem function following the invasion of EAB.

Changes in the canopy, understory vegetation communities, water-level, and soil temperature may lead to altered biogeochemical cycling and potential nutrient loss from black ash wetlands to the atmosphere and down-stream ecosystems following EAB invasion. The gaseous fluxes of carbon (as CO<sub>2</sub> and CH<sub>4</sub>) and nitrogen (N<sub>2</sub>O) as greenhouse

\* Corresponding author.

E-mail addresses: [toczy003@umn.edu](mailto:toczy003@umn.edu) (A.J.Z. Toczydlowski), [raslesak@umn.edu](mailto:raslesak@umn.edu) (R.A. Slesak), [rkolka@fs.fed.us](mailto:rkolka@fs.fed.us) (R.K. Kolka), [rod.venterea@usda.gov](mailto:rod.venterea@usda.gov) (R.T. Venterea).

<https://doi.org/10.1016/j.apsoil.2020.103565>

Received 13 August 2019; Received in revised form 14 February 2020; Accepted 19 February 2020

0929-1393/© 2020 Elsevier B.V. All rights reserved.

gasses are measurable indicators of how changes in ecosystem dynamics will alter nutrient cycling and ecosystem function. Greenhouse gas fluxes are controlled by the abundance and productivity of microbial populations in the soil, which are regulated by several factors including temperature, organic matter, and the availability of electron donors and acceptors needed to complete the oxidation-reduction reactions of metabolic processes under aerobic and anaerobic conditions (Altshuler et al., 2019; Ebrahimi and Or, 2016; Hou et al., 2000). The availability of electron donors can also limit nutrient cycling reactions in the soil and therefore gas production (Wang et al., 1993). For example, denitrification requires a soluble carbon electron donor and nitrification uses ammonium as an electron donor. A noticeable shift in Eh and gas fluxes will only occur if soil microbes have an abundant food source (soil organic matter), abundant electron donors and acceptors to complete metabolic reactions, and an environment warm enough to be biologically active. Given the above, it is necessary to understand how soil temperature and degree of soil saturation affect gas fluxes in black ash wetlands with different hydroperiods and soil composition (i.e., mineral vs. organic soils).

Van Grinsven et al. (2018) measured soil CO<sub>2</sub> and CH<sub>4</sub> fluxes in black ash wetlands with simulated EAB disturbance in Upper Michigan. The disturbance resulted in significantly higher CO<sub>2</sub> fluxes, largely because the disturbed sites had elevated soil temperatures due to increased solar radiation with canopy loss. The average CH<sub>4</sub> fluxes in disturbed sites were not significantly different from the control sites, but larger CH<sub>4</sub> fluxes did occur more frequently in disturbed sites. Overall, changes in soil temperature and moisture regulated the soil carbon fluxes, producing significant treatment effects. In northern Minnesota, simulated EAB disturbance in black ash wetlands resulted in warmer air temperatures, but soil gas fluxes were not evaluated (Slesak et al., 2014). The differences in hydrology and soil composition between the black ash wetlands studied in Upper Michigan, and those in other regions of the Great Lakes states will likely result in different gaseous carbon flux responses following EAB induced ash dieback.

Field experiments simulating EAB-induced ash mortality in black ash wetlands in northern Minnesota and Upper Michigan have measured changes in water table, understory plant communities, soil temperature, and nutrient cycling (Davis et al., 2017; Looney et al., 2015; Slesak et al., 2014; Telander et al., 2015; Van Grinsven et al., 2017, 2018). Other studies and literature reviews suggest EAB will cause changes in ash foliar chemistry, invertebrate communities, and trophic interactions that will cascade through entire ecosystems (Chen et al., 2011; Nisbet et al., 2015; Perry and Herms, 2016; Youngquist et al., 2017). However, many hypothesized impacts of emerald ash borer on forested wetlands are still uncertain, and there is an urgent need to understand the cascading impacts of EAB on ecosystem processes such as greenhouse gaseous efflux. We used a soil core incubation experiment that mimicked potential future hydrologic and temperature regimes to investigate the interactions among water-level, soil temperature, soil oxidation-reduction potential (redox), and greenhouse gas (CO<sub>2</sub>, CH<sub>4</sub>, and N<sub>2</sub>O) fluxes in black ash wetland soils in the Great Lakes region to determine if: (1) warmer soil temperatures will result in greater greenhouse gas fluxes, (2) higher water levels will increase greenhouse gas fluxes, and if so, (3) there is an interaction with soil temperature that amplifies the water table response, and (4) the response differs between mineral and peat soils. This study builds on previous research studying a critical system of feedbacks facing the imminent threat of emerald ash borer invasion and a cascade of ecosystem-scale changes (Davis et al., 2017; Looney et al., 2015; Slesak et al., 2014; Van Grinsven et al., 2018, 2017).

## 2. Methods

### 2.1. Study area

Intact soil cores were collected from black ash wetlands with

mineral and organic, peat soils in northern Minnesota and Upper Michigan, respectively. The northern Minnesota site with mineral soils was an undisturbed area adjacent to treatment plots presented in the Slesak et al. (2014) and Looney et al. (2015) studies. The study site is located in the Chippewa National Forest in northern Minnesota's Itasca County (N47.5°, W94°) and has a continental climate with a mean growing season (May–Oct.) temperature of 14.3 °C (Slesak et al., 2014). The wetlands occur on poorly to very poorly drained soils with either loam to sand textures derived from glacio-fluvial parent material, or clay to silty clay texture formed from glacio-lacustrine parent material overlain with approximately 30 cm of muck (Slesak et al., 2014). Most of the wetlands are underlain by a hydrologic confining layer of lacustrine clay at a depth of 10–150 cm. The forest composition is primarily black ash (75%–100% basal area) (Slesak et al., 2014).

The organic, peat soil cores were collected from an undisturbed black ash headwater wetland similar, and in close proximity to those studied by Van Grinsven et al. (2017) and Davis et al. (2017) in the western Upper Peninsula of Michigan, on the Ottawa National Forest in Ontonagon County (N46.5°, W89°). The wetlands are dominated by black ash (*F. nigra*) (40%–95% basal area) and occur in topographic depressions that experience seasonal inundation and commonly have distinct surface drainage outlets. Soils at this site are woody peat Histosols with peat depths ranging from 40 cm to > 690 cm, with an average depth of 140 cm (Van Grinsven et al., 2017). The peat has a distinct vertical gradient of physical properties including a shallow hydrologically active layer and a deeper, nearly impermeable layer restricting water movement below 30 cm depth. There is commonly a lens of clay or poorly sorted clay-loam underlying the peat.

### 2.2. Soil core collection and storage

A total of 60 intact soil cores were collected from the northern Minnesota and Upper Michigan field sites in early November 2016. At each site, 30 cores were positioned in a grid pattern with approximately three-meter spacing between cores. Vegetation and fresh leaf litter were removed before collecting each core. The cores were extracted from the soil profile using 50-cm lengths of 10-cm diameter schedule 40 polyvinyl chloride (PVC) pipe (10.1 cm inside diameter), which were pounded into the wetland with a sledgehammer until nearly flush with the soil surface, then removed and sealed on the bottom with a rubber cap and hose clamp. Soil compaction in the cores was measured as the elevation difference between soil surface inside and outside of the cores. The average soil compaction was 2.7 cm in the mineral soil cores and 4.5 cm in the peat cores, increasing the bulk density by about 6% and 10% respectively (Table 1). Variation in soil compaction led to variable headspaces in the cores which was accounted for in all gas flux measurements described below. The average headspace was 4.6 cm and 4.7 cm in cores from the mineral soil and peat soil sites respectively.

Nearby surface water, referred to as “source water”, was collected in polycarbonate carboys from each field site at the same time as soil core collection to add to the cores throughout the experiment. The water carboys and soil cores were stored vertically for approximately three months at a mean temperature of 3.6 °C before the experiment to reduce microbial activity in the soil. The soil cores were stored with antecedent soil water contents; nearly saturated (estimated 80%) for the mineral soils and saturated for the peat soil cores, many with standing surface water.

### 2.3. Incubation experiment design and setup

The experiment was a two-way factorial design with two water-level treatments (saturated and drawdown), and three incubation temperatures (10 °C, 15 °C, and 20 °C) for each soil type (site). Treatments were randomly assigned with five replicate cores per treatment. The saturated cores, designed to mimic a wetland post-EAB infestation, had the water level maintained at the soil surface for the duration of the

**Table 1**

Soil core properties.

Summary of select physical and chemical properties of the soil cores by soil type. Soil properties were measured on entire incubated cores ( $n = 30$  per soil type), destructively sampled and oven dried (mineral soils at 105 °C and peat at 65 °C) following the experiment. Standard error in parentheses.

Soil core property	Mineral soil cores	Peat cores
Soil compaction during core collection (cm)	2.7 (0.2)	4.5 (0.4)
A-horizon depth (cm)	5.4 (0.2)	na
Total dry mass (g)	5246 (39)	513 (16)
Coarse fraction > 2 mm (g)	0.2 (0.1)	na
Woody roots (g)	11.1 (0.9)	14.6 (1.2)
Undecomposed wood (g)	0.5 (0.3)	19.4 (2.6)
Concretions (g)	39.1 (11.3)	na
pH (0–15 cm) <sup>a</sup>	4.7 (0.1)	4.4 (0.0)
Soil carbon (%) <sup>b</sup>	0.9 (0.1)	51.2 (0.4)
Soil nitrogen (%) <sup>b</sup>	0.1 (0.0)	2.4 (0.0)
Phosphorus ( $\text{mg kg}^{-1}$ ) <sup>c</sup>	36 (2)	na
Bulk density ( $\text{Mg m}^{-3}$ )	1.5 (0.0)	0.15 (0.0)

<sup>a</sup> Soil pH was measured with a glass electrode in a 2:1 water to soil slurry.

<sup>b</sup> Total soil C and N were measured via dry combustion.

<sup>c</sup> Total soil P was determined via Bray extraction and spectrophotometry.

experiment. The drawdown cores had variable water levels throughout the experiment simulating the seasonal drawdown of an undisturbed wetland as measured in northern Minnesota (Slesak et al., 2014). The drawdown cores were initially saturated, then drawn down in 15-cm increments weekly, the water level reaching 45 cm below the soil surface in the fourth week. The drawdown cores were then re-saturated, and the 4-week incremental drawdown sequence was repeated once over the second half of the experiment. The soil cores were incubated in parallel in three 1.5 m<sup>2</sup> environmental growth chambers (model E15, Controlled Environments LTD., Canada) at 10 °C, 15 °C, or 20 °C for eight weeks (56 days). Each chamber was outfitted with four temperature sensors (iButton® Embedded Data Systems LLC, Lawrenceburg, KY, USA) logging at 15-minute intervals, one adhered to each chamber wall, and a single sensor (HOBO® U23 Pro v2 External Temperature/Relative Humidity Data Logger, MA, USA) was suspended from the ceiling and, recorded relative humidity and temperature at 10-minute intervals. The mean temperatures recorded by the probes over the duration of the experiment were 11.1 °C, 15.7 °C, and 20.3 °C for the 10 °C, 15 °C, and 20 °C chambers, respectively, with corresponding mean relative humidity values of 47.6%, 42.3%, and 42.0%.

Drawdown cores were fitted with three brass, barbed hose fittings

through the side of the PVC at 15 cm, 30 cm, and approximately 42–45 cm (as close to the bottom as possible) below the soil surface (Fig. 1). Saturated cores received only the bottom-most fitting. Each core was placed on a wooden riser to normalize soil surface elevation and connected to a reservoir filled with source water used to maintain water levels in the cores (Fig. 1). On average, 54 ml of source water was added to the soil surface of each saturated core, each week, to replace water lost to evaporation.

Platinum redox electrodes were inserted into all cores to monitor redox potential throughout the experiment. Each core received three electrodes, inserted vertically to depths of 15 cm, 30 cm, and approximately 42 cm below the soil surface that remained in place for the duration of the experiment (Fig. 1). The redox electrodes were designed, constructed, and tested in-house based on published techniques (Fiedler et al., 2007; Hinchey and Schaffner, 2005; Scholz, 2010). The electrodes were tested against a silver silver-chloride (Ag-AgCl), 1.00 M potassium chloride (KCl) reference electrode (model CHI11, CH Instruments Inc., TX, USA) in the strongly oxidizing, standard ferrous-ferric solution described by Light (1972) with a mean Eh of 408 mV with 9.2 mV standard deviation; electrodes with values furthest from the accepted value, 439 mV were discarded.

#### 2.4. Samples and measurements

The soil cores were allowed six days to acclimate to chamber conditions, then all 60 cores were saturated to the surface with source water seven days before the first measurements. Gas samples were collected weekly (seven days after each water-level change), to monitor CO<sub>2</sub>, CH<sub>4</sub>, and N<sub>2</sub>O fluxes, redox was measured twice per week, and pore water samples were collected passively during the water-level drawdowns when drainage volumes were sufficient.

Gas fluxes were quantified weekly based on published methods (Berryman et al., 2009; De Klein and Harvey, 2012). For gas sampling, a PVC cap was placed on the top of each core and 12-mL samples were collected via syringe at 0, 10 and 20 min after placing the cap. The PVC caps were vented to avoid pressure perturbations in the sample headspace during placement. Gas samples were immediately transferred to 9-ml glass vials sealed with butyl rubber septa and analyzed within 48 h using two gas chromatographs (Agilent/Hewlett-Packard, Palo Alto, CA), one equipped with a thermal conductivity detector to measure CO<sub>2</sub> and an electron capture detector for N<sub>2</sub>O, and the other equipped with a flame ionization detector to measure CH<sub>4</sub>, both connected to a headspace auto-sampler (Teledyne Tekmar, Mason, OH). A 14-port valve

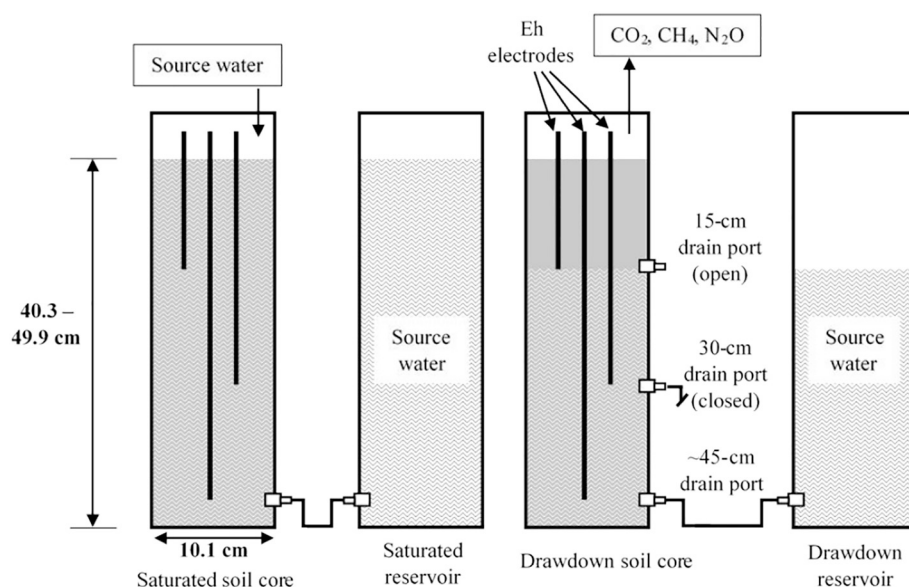


**Fig. 1.** Schematic of one saturated soil core, one drawdown soil core, their plumbing, water-level control reservoir system, and platinum redox (Eh) electrodes. The cores were 4-inch (10.1 cm) diameter schedule 40 PVC, 50 cm long. Drawdown cores were fit with three brass fittings; saturated cores with one. Cores in each treatment group ( $n = 5$ ) were connected to a single reservoir filled with “source water” from the corresponding field site. For this schematic the drawdown core is shown at the 15-cm drawdown depth. Each core received three, permanent Eh electrodes inserted vertically to depths of 15 cm, 30 cm, and approximately 42 cm.

(Valco Instruments, Houston, TX) split each gas sample into three separate sample loops. Gas fluxes were calculated using the rate of change in gas concentration, the headspace volume for each soil core (approximately 0.0007 m<sup>3</sup>), and soil surface area (0.0080 m<sup>2</sup>).

Soil redox potential was measured two days and six days after each water-level change. To measure Eh, the Ag-AgCl reference electrode was inserted into the soil surface in the center of the core to an approximate depth of three cm. Positive and negative leads from an auto range digital multimeter (Radio Shack, Fort Worth, TX) were clipped to the exposed copper end of a platinum redox electrode and the reference electrode respectively. Redox values were recorded when the multimeter reading stabilized for 5 s.

### 2.5. Statistical analyses

All statistical analyses were completed using R statistical software (R Core Team, 2017) and conducted individually for each soil type (site). Repeated measures analysis was used to assess periodic data with the 'nlme' R package (Pinheiro et al., 2017). When treatment effects were found, differences among treatment combinations were tested using least-squared means (LSM) analyses with the 'lsmeans' R package (Lenth, 2016). The experimental design did not allow us to test for chamber effects described by Hammer and Hopper (1997) because only one individual growth chamber was used for each temperature treatment. However, the rigorous monitoring of temperature and relative humidity in each chamber showed there was likely no inherent differences based on the mechanics or historical use of the environmental chambers used in this experiment (Toczylowski, 2018), so statistical comparisons were made among chambers (i.e., temperature treatments). The "powerTransform" tool from the 'car' R package was used to identify the most appropriate data transformation when needed to stabilize the variance (Fox and Weisberg, 2011).

For CO<sub>2</sub>, flux values were log transformed to stabilize variance. For CH<sub>4</sub> and N<sub>2</sub>O, flux values were adjusted to convert negative values into positive values and transformed by (Flux + 1)<sup>-10</sup> and (Flux + 1)<sup>-0.8</sup> respectively, to stabilize variance. Un-transformed means and standard error are presented in figures for display purposes. Gas fluxes were analyzed separately for each soil type using repeated measures models with temperature, water-level, and sample week as fixed factors, and an auto regressive level (1) (AR[1]) covariance matrix (Pinheiro et al., 2017). We also explored analysis of covariance (ANOVA) using core-specific characteristics as potential covariates (bulk density, root mass, undecomposed wood mass, organic horizon depth, soil core depth, core mass, fine soil fraction mass, and mass of soil concretions [Table 1]), but model performance was not greatly improved, and covariates were not included in any model. Treatment effects with interactions were tested using a three-way ANOVA and LSM test (Lenth, 2016).

Cumulative gas fluxes over the duration of the experiment were calculated using trapezoidal integration. To stabilize the variance, cumulative CO<sub>2</sub> and CH<sub>4</sub> fluxes were log transformed, and N<sub>2</sub>O fluxes were transformed by a power of -1. Cumulative fluxes were modeled separately for mineral and peat soils using simple linear regression with temperature and water-level as predictors. Treatment effects were tested using two-way ANOVA and LSD tests (de Mendiburu, 2017).

To express soil redox potential relative to the standard hydrogen electrode, Eh measured using a Ag-AgCl reference electrode at 10 °C, 15 °C, or 20 °C were adjusted by +244.4 mV, +241.8 mV, or +239.6 mV respectively (Kahlert, 2010). Redox measurements were averaged across depths within each soil core for all analyses. Redox was modeled separately by soil type using repeated measures analysis with an AR(1) correlation structure and temperature treatment, water-level treatment, and sample day as predictors. The same covariates tested in the gas flux models were examined for the redox models with a similar result, so no covariates were included in the redox models. Treatment effects with interactions were tested using a three-way ANOVA and LSM test (Lenth, 2016).

The interaction of redox with gas fluxes was analyzed using multiple linear regression and ANOVA to compare models with fixed-intercept/fixed-slope, fixed-intercept/variable-slope, variable-intercept/fixed-slope, and variable-intercept/variable-slope. Since redox was monitored twice per week and gas fluxes only once, the redox values from the day prior were paired with gas flux measurements and the other redox measurements were disregarded for this analysis. The gas flux values were adjusted to convert negative values into positive values to allow for transformation of the data to stabilize variance. The transformations used were (Flux)<sup>0.25</sup>, (Flux + 1)<sup>-9</sup>, and (Flux + 1)<sup>-0.9</sup> for CO<sub>2</sub>, CH<sub>4</sub>, and N<sub>2</sub>O, respectively. The best models were selected based on the Akaike information criterion (AIC), residual standard error, r-squared value, F-statistic, and p-value and confirmed using ANOVA to compare models.

## 3. Results

### 3.1. Gas flux response

In soils from both sites, gas fluxes were generally greatest in the 20 °C treatment, and fluxes were commonly near zero in the 10 °C treatment (Fig. 2). Temporal trends were most apparent in the saturated treatment at 20 °C, where fluxes increased over the course of the incubation experiment. As the experiment progressed, the gas fluxes became more variable as indicated by increasing standard error in each measurement period, especially in the 20 °C treatments and for CH<sub>4</sub> fluxes. Significant treatment effects were observed for all gas species in the mineral soil and for CO<sub>2</sub> and CH<sub>4</sub> in the peat soil (Table 2). Three-way, temperature by water-level by week interactions were significant only for CO<sub>2</sub> and CH<sub>4</sub> in the mineral soil.

#### 3.1.1. Carbon dioxide

In mineral soil from northern Minnesota, a significant three-way, temperature by water-level by week interaction effect for daily CO<sub>2</sub> flux was likely driven by differences between water-level treatments in week two and temperature treatments throughout the experiment (Table 2, Fig. 2a). Multiple comparisons indicated that in most weeks, daily fluxes were greater at 20 °C than at 10 °C or 15 °C within a water-level treatment and that water-level treatment effects occurred in the 10 °C treatments in weeks two and eight, and in the 15 °C treatments in week two, the drawdown treatment being greater in all three instances. The cumulative CO<sub>2</sub> flux data indicated a significant temperature by water-level interaction effect (Table 2), where cumulative fluxes generally increased with temperature, and also differed among water level treatments at 15 °C (Table 3). Overall, the greatest mean cumulative CO<sub>2</sub> flux was 98 g C m<sup>-2</sup> in the saturated treatment at 20 °C.

In the peat soil from Upper Michigan, a significant interaction of water-level and week occurred because daily CO<sub>2</sub> fluxes were 28% to 187% greater in the drawdown treatment in weeks two, three, and seven, but greater in the saturated treatment by 49% in week five (Table 2, Fig. 2b). The main effect of temperature was significant with the 10 °C, 15 °C, and 20 °C treatments all differing with mean daily CO<sub>2</sub> fluxes of 0.83, 0.92, and 1.86 g C m<sup>-2</sup> day<sup>-1</sup>, respectively (Table 2). This effect of temperature was also reflected in the cumulative flux data, as the 20 °C treatment had greater cumulative CO<sub>2</sub> flux than the 10 °C and 15 °C treatments. Water-level was also a significant factor for cumulative CO<sub>2</sub> with the drawdown treatment having 28% percent greater flux than the saturated treatment (Table 3).

#### 3.1.2. Methane

For CH<sub>4</sub> in the mineral soil cores, there was a three-way interaction with significantly greater daily fluxes in the saturated treatment at 20 °C than all other treatments in week four and beyond. This effect became more pronounced over time, with fluxes ranging from about 100% to 300% greater by week eight, but daily fluxes were still relatively low overall (< 0.15 g C m<sup>-2</sup> day<sup>-1</sup>) (Fig. 2c). Cumulative CH<sub>4</sub>

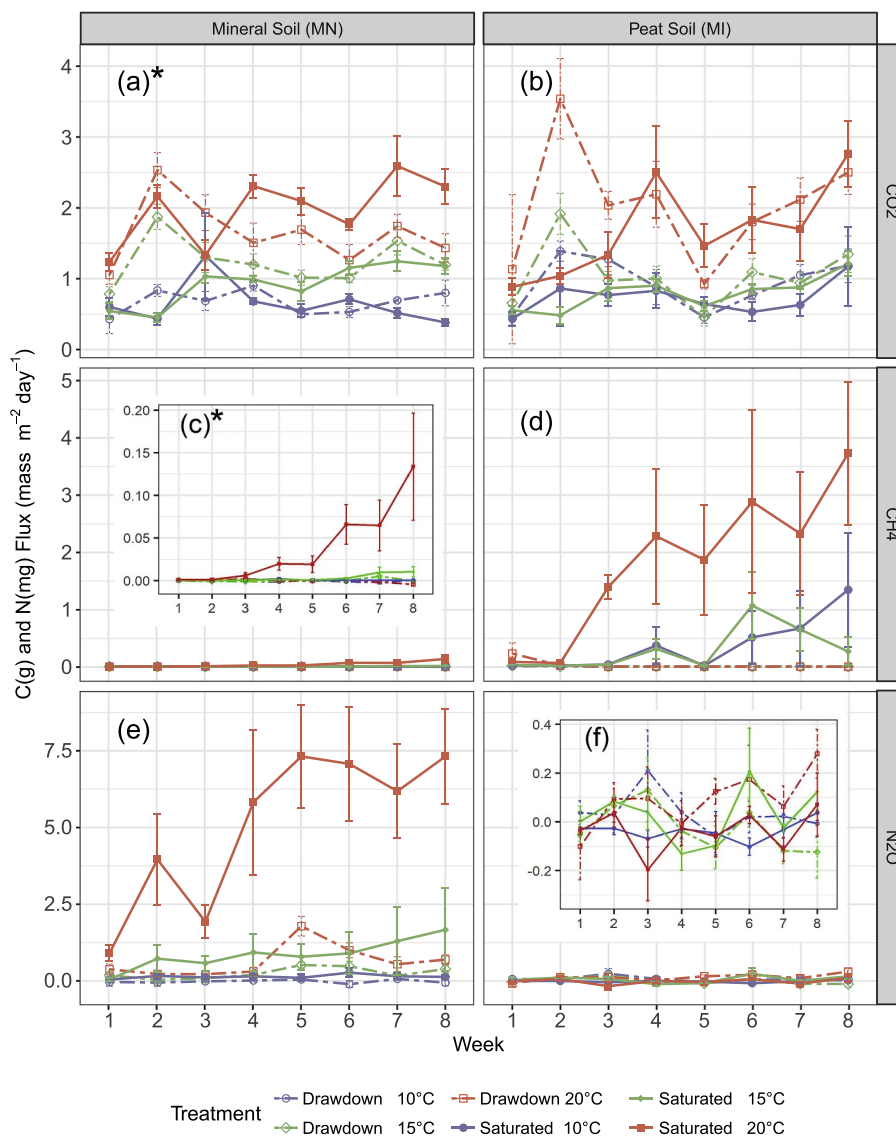


**Fig. 2.** Treatment means of un-transformed gas fluxes. Error bars show standard error. The mineral soil  $\text{CH}_4$  (c) and peat soil  $\text{N}_2\text{O}$  (f) panels include inset graphs above the data with larger scales to clearly show trends. Asterisks (\*) indicate panels with significant ( $p < 0.1$ ) three-way, temperature by water-level by week interactions. Note:  $\text{N}_2\text{O}$  fluxes are in  $\text{mg N m}^{-2} \text{day}^{-1}$ ,  $\text{CO}_2$  and  $\text{CH}_4$  are in  $\text{g C m}^{-2} \text{day}^{-1}$ .

flux estimates reflected the daily treatment effects, with a maximum of  $1.7 \text{ g C m}^{-2}$  for the saturated-20 °C treatment and negligible fluxes ( $< 0.14 \text{ g C m}^{-2}$ ) in all remaining treatments.

The  $\text{CH}_4$  fluxes displayed the most visually apparent treatment effects in the peat soil cores (Fig. 2d). There were significant water-level by week interaction effects (Table 2) with greater fluxes in the saturated treatment than in the drawdown treatment in week three and beyond that ranged from  $0.49 \text{ g C m}^{-2} \text{day}^{-1}$  in week three to  $1.78 \text{ g C m}^{-2} \text{day}^{-1}$  in week eight. There was also a significant temperature by water-level interaction and pairwise comparisons indicated that each saturated treatment had significantly greater daily  $\text{CH}_4$  fluxes than every drawdown treatment, and that the saturated treatment at 20 °C was greater than all other treatment combinations by 1.45 to  $1.82 \text{ g C m}^{-2} \text{day}^{-1}$ . Within each temperature treatment, daily fluxes were 60 to 135 times greater in the saturated treatment than the corresponding drawdown treatment. Within the drawdown treatment,  $\text{CH}_4$  flux did not differ by temperature. Similar trends were apparent in the cumulative  $\text{CH}_4$  fluxes with significant temperature and water-level factors (Table 2). The 20 °C treatment had significantly (approximately 5.6 times) greater cumulative fluxes than both the 10 °C and 15 °C

treatments and the saturated treatment was 105 times greater than the drawdown treatment (Table 3).

### 3.1.3. Nitrous oxide

The most visually apparent treatment effects in the mineral soil cores were in the  $\text{N}_2\text{O}$  fluxes (Fig. 2e), where there was a significant temperature by water-level interaction effect (Table 2). The mean daily flux in the saturated treatment at 20 °C was 6 to 46 times greater than all other treatments. This trend did not vary over time, but week is a significant factor in the model (Table 2) because the flux in week one was significantly less than the flux in weeks five through eight. Similar findings were observed for cumulative  $\text{N}_2\text{O}$  flux, where the saturated treatment at 20 °C produced  $253.7 \text{ g N m}^{-2}$ , 8 to 43 times more than other treatments (Table 3). Relative to mineral soil, peat soil produced minimal  $\text{N}_2\text{O}$  fluxes ( $< 0.28 \text{ mg N m}^{-2} \text{day}^{-1}$ ) regardless of treatment (Fig. 2f). There was a significant temperature by water-level interaction effect in the daily  $\text{N}_2\text{O}$  flux model (Table 2), but pairwise comparisons did not reveal any significant differences among treatments. There was also a significant temperature by water-level interaction effect for the cumulative  $\text{N}_2\text{O}$  fluxes (Table 2), but again no pairwise differences were detected (Table 3).

**Table 2**

ANOVA results for gas flux models.

Summary of F-statistic probabilities and degrees of freedom for three-way ANOVA results for gas flux models (top) and two-way ANOVA results for cumulative gas flux models (bottom).

Model term	Num DF	CO <sub>2</sub>	CH <sub>4</sub>	N <sub>2</sub> O
		p-Value	p-Value	p-Value
<b>Gas flux model results</b>				
<b>Mineral soil</b>				
Temp	2	< 0.0001	< 0.0001	< 0.0001
Water	1	0.1553	< 0.0001	< 0.0001
Week	7	< 0.0001	< 0.0001	0.0002
Temp:water	2	< 0.0001	< 0.0001	< 0.0001
Temp:week	14	0.0203	< 0.0001	0.2633
Water:week	7	< 0.0001	< 0.0001	0.1573
Temp:water:week	14	0.0005	< 0.0001	0.7327
<b>Peat soil</b>				
Temp	2	< 0.0001	< 0.0001	0.9492
Water	1	0.0015	< 0.0001	0.1614
Week	7	< 0.0001	0.0030	0.3079
Temp:water	2	0.4419	< 0.0001	0.0390
Temp:week	14	0.6620	0.6263	0.1527
Water:week	7	< 0.0001	< 0.0001	0.1536
Temp:water:week	14	0.9618	0.1084	0.5033
<b>Cumulative gas flux model results</b>				
<b>Mineral soil</b>				
Temp	2	< 0.0001	< 0.0001	< 0.0001
Water	1	0.3767	< 0.0001	< 0.0001
Temp:water	2	0.0128	< 0.0001	0.0129
<b>Peat soil</b>				
Temp	2	< 0.0001	0.0370	0.8754
Water	1	0.0120	< 0.0001	0.1556
Temp:water	2	0.9194	0.4334	0.0383

### 3.2. Soil redox potential

Soil redox potential displayed significant water-level by day and temperature by water-level interaction effects for both mineral and peat soils, but no three-way interactions were significant (Table 4). In the mineral soil, water-level had a significant effect on Eh on five sample days during the first drawdown period, then again on three sample days

**Table 3**

Cumulative gas fluxes and mean redox by treatment.

Cumulative gas fluxes and mean redox (Eh) by treatment group. Lowercase letters (a) denote significant ( $p < 0.1$ ) differences among treatments within soil types where either significant main effects or interaction effects were identified (Table 2), based on transformed values. Standard error is shown in parentheses.

Treatment	CO <sub>2</sub>	CH <sub>4</sub>	N <sub>2</sub> O	Eh
	g C m <sup>-2</sup>	g C m <sup>-2</sup>	Mg N m <sup>-2</sup>	mV
<b>Mineral soil</b>				
Saturated 10 °C	32.89 (4.3) a	0.03 (0.01) a	5.96 (3.7) abc	-206 (3) a
Drawdown 10 °C	33.25 (0.9) a	-0.05 (0.01) a	-1.94 (1.1) a	-194 (7) ad
Saturated 15 °C	45.86 (1.5) b	0.14 (0.07) a	41.28 (21.2) bc	-224 (4) b
Drawdown 15 °C	62.43 (5.4) c	0.01 (0.04) a	11.15 (2.1) abc	-171 (7) c
Saturated 20 °C	98.19 (3.9) d	1.71 (0.50) b	253.7 (61.8) d	-209 (3) ab
Drawdown 20 °C	83.42 (7.2) d	-0.01 (0.03) a	31.05 (5.8) bc	-183 (9) cd
<b>Peat soil</b>				
Saturated 10 °C	40.94 (3.6) a <sup>†</sup>	8.12 (5.0) a <sup>†</sup>	-2.12 (1.2) a	-188 (2) a
Drawdown 10 °C			1.88 (1.9) a	-107 (11) b
Saturated 15 °C	44.97 (3.1) a <sup>†</sup>	7.87 (4.64) a <sup>†</sup>	0.95 (1.0) a	-189 (2) a
Drawdown 15 °C			-0.83 (1.8) a	-155 (9) c
Saturated 20 °C	1.45 (9.9) b <sup>‡</sup>	44.90 (19.8) b <sup>‡</sup>	-2.20 (0.8) a	-189 (3) a
Drawdown 20 °C			4.42 (2.5) a	-157 (8) c
Saturated	51.87 (7.2) a <sup>‡</sup>	40.21 (13.2) a <sup>‡</sup>	na	na
Drawdown	66.37 (8.2) b <sup>‡</sup>	0.38 (0.2) b <sup>‡</sup>	na	na

<sup>†</sup> These cumulative fluxes are grouped by temperature treatment only, because the water-level by temperature interactions were not significant, but the main effect of temperature was.

<sup>‡</sup> These cumulative fluxes are grouped by water-level treatment only, because the water-level by temperature interactions were not significant, but the main effect of water-level was.

**Table 4**

ANOVA results for redox models.

Summary of F-statistic probabilities and degrees of freedom for three-way ANOVA results for the soil redox models.

Model term	Num DF	Mineral soil	Peat soil
		p-Value	p-Value
Temp	2	0.6805	< 0.0001
Water	1	< 0.0001	< 0.0001
Day	7	< 0.0001	< 0.0001
Temp:water	2	0.0001	< 0.0001
Temp:day	14	0.2147	0.8836
Water:day	7	< 0.0001	< 0.0001
Temp:water:day	14	0.1230	0.8687

during the second drawdown period (Fig. 3). Pairwise comparisons indicated that Eh was 31% and 15% more negative in the saturated than the drawdown treatments at 15 °C and 20 °C respectively, but did not differ at 10 °C (Table 3). In general, for the mineral soil, periods in the drawdown treatment associated with a longer duration of unsaturated conditions had more positive redox potential compared to saturated treatments.

In the peat soil, redox responded more consistently to both temperature and water-level treatments than mineral soil. There were significant water-level effects on Eh on four sample days of the first drawdown period, and on another four sample days during the second drawdown (Fig. 3). The temperature by water-level interaction effect manifested as Eh values were 21% to 75% more negative in the saturated than the drawdown treatment at all temperatures, and the drawdown treatment at 10 °C was significantly less negative than either the 15 °C or 20 °C drawdown treatments. There were no differences among temperatures in the saturated treatments (Table 3).

### 3.3. Gas flux-redox interactions

When modeled as the sole predictor of gas fluxes, Eh explained very little of the variance in gas fluxes ( $r^2$  values ranged from 0.001 to 0.057). When temperature and water-level treatment factors were included, the best models were greatly improved and had  $r^2$  values

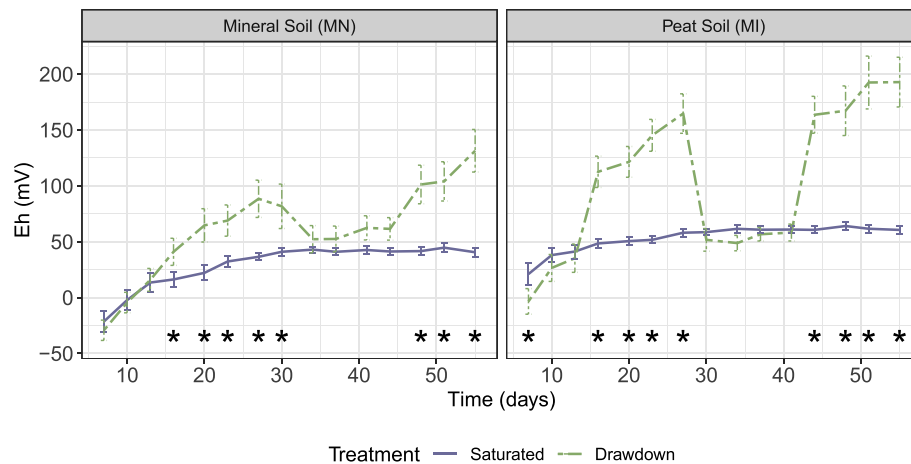


**Fig. 3.** Mean soil redox potential (Eh) by water-level treatment. Error bars show standard error. Asterisks (\*) indicated days with significant ( $p < 0.1$ ) differences between treatments.

**Table 5**

Summary statistics for redox-gas flux models.

Summary statistics for the best redox-gas flux models for each soil type and gas species.

Gas	Intercept	Slope	R <sup>2</sup>	F-Stat	p-Value
Mineral soil					
CO <sub>2</sub>	Variable	Variable	0.57	27.34	< 0.0001
CH <sub>4</sub>	Variable	Variable	0.41	14.13	< 0.0001
N <sub>2</sub> O	Variable	Variable	0.60	30.82	< 0.0001
Peat soil					
CO <sub>2</sub> <sup>a</sup>	Variable	Fixed	0.30	16.52	< 0.0001
CH <sub>4</sub>	Variable	Variable	0.58	28.12	< 0.0001
N <sub>2</sub> O <sup>b</sup>	Fixed	Variable	0.05	1.96	0.0725

<sup>a</sup> For CO<sub>2</sub> in the peat soil, there was no significant difference between the variable-intercept/variable-slope and variable-intercept/variable-slope models ( $p = 0.76$ ).

<sup>b</sup> For N<sub>2</sub>O in the peat soil, there was no significant difference among any of the four models; the model with the lowest p-value was selected.

ranging from 0.3 to 0.6, except for N<sub>2</sub>O fluxes in the peat soil ( $r^2 = 0.05$ ) (Table 5). In Fig. 4 it is apparent the production of CH<sub>4</sub> and N<sub>2</sub>O is limited to specific ranges of Eh. In the peat soil, all CH<sub>4</sub> fluxes  $> 0.25 \text{ g C m}^{-2} \text{ day}^{-1}$  occur in the Eh range 0 to 100 mV (Fig. 4d). In the mineral soil, 87% of N<sub>2</sub>O fluxes  $> 1 \text{ mg N m}^{-2} \text{ day}^{-1}$  occur in the Eh range 0 to 55 mV (Fig. 4e). When gas fluxes are large, there is generally a positive relationship with Eh, especially at 20 °C (Fig. 4). However, inferences about Eh and greenhouse gas fluxes are limited because Eh measurements are temporally variable and were taken the day prior to gas flux measurements.

#### 4. Discussion

Forested black ash wetlands in the Great Lakes region are especially threatened by the impending invasion of EAB because the ash-dominated canopies control the local groundwater levels via transpiration (Telander et al., 2015) and loss of ash from the canopy will result in higher water table levels and warmer air temperatures (Slesak et al., 2014; Van Grinsven et al., 2017). This laboratory experiment shows that black ash wetlands in northern Minnesota and Upper Michigan with mineral and peat soils respectively, will both likely experience altered biogeochemical cycling and an increase in greenhouse gases production with higher water table levels resulting from EAB disturbance. In particular, N<sub>2</sub>O fluxes increased in the mineral soil and CH<sub>4</sub> fluxes increased in the peat soil under saturated and warm conditions, in addition to variable effects on CO<sub>2</sub>.

#### 4.1. Carbon dioxide

In both mineral and peat soils, CO<sub>2</sub> fluxes were similar between water-level treatments. In the peat soil, drawdown treatments had significantly greater mean CO<sub>2</sub> fluxes than saturated treatments in some weeks, but the opposite response was observed in others. This inconsistency was reflected in the cumulative flux estimates, where the differences between water-level treatments were small (Table 3). Because CO<sub>2</sub> is a byproduct of aerobic respiration, we hypothesized that the drawdown treatments would release more CO<sub>2</sub> than the saturated treatments when the water level was below the soil surface. Van Grinsven et al. (2018) measured in-situ CO<sub>2</sub> fluxes in Upper Michigan and reported fluxes of similar magnitude to those measured in our study, which increased as the water table level decreased, and soil temperature increased, as expected. However, the soil cores in our experiment, among other artifacts, did not include vegetation, and therefore lacked the production of CO<sub>2</sub> via root respiration compared to the vegetated plots measured by Van Grinsven et al. (2018). Other research has also shown CO<sub>2</sub> fluxes increasing as wetland soils are drained (DeBusk and Reddy, 2003; Smith et al., 2003; Yang et al., 2013).

In intact soil core incubation experiments, Chen et al. (2019) measured CO<sub>2</sub> fluxes of a similar magnitude at 20 °C in wetland soils from temperate, continental China, noting increased fluxes following wetting in simulated rainfall events, and Doroski et al. (2019) measured much smaller CO<sub>2</sub> fluxes in saturated soil cores from the coastal United States. However, Doroski et al. (2019) used soil cores inundated with 2.5 cm of stagnant water over the soil surface and the incubation temperature was not reported. Similar to our results, Berryman et al. (2009) did not see a CO<sub>2</sub> response to water-level treatments in intact soil cores from a calcareous wetland in western Minnesota with fluxes of a similar magnitude. They attributed the lack of a net CO<sub>2</sub> response to methane oxidation in the upper soil column (Berryman et al., 2009), meaning CH<sub>4</sub> produced lower in the soil column was oxidized and released to the atmosphere as CO<sub>2</sub>. Methane production and subsequent oxidation to CO<sub>2</sub> could also have been a factor in our experiment because drawdown cores would still have areas of anaerobic (as well as aerobic) conditions throughout the course of the experiment.

The effect of temperature on CO<sub>2</sub> fluxes was more straightforward, as both daily and cumulative fluxes increased with temperature as expected. Carbon dioxide fluxes generally increase exponentially as temperature increases unless soil water content is a limiting factor (Smith et al., 2003). Despite the inconsistent water-level treatment response for CO<sub>2</sub>, our results indicate that any increase in soil temperature following EAB disturbance in black ash wetlands would lead to an increase in CO<sub>2</sub> fluxes.

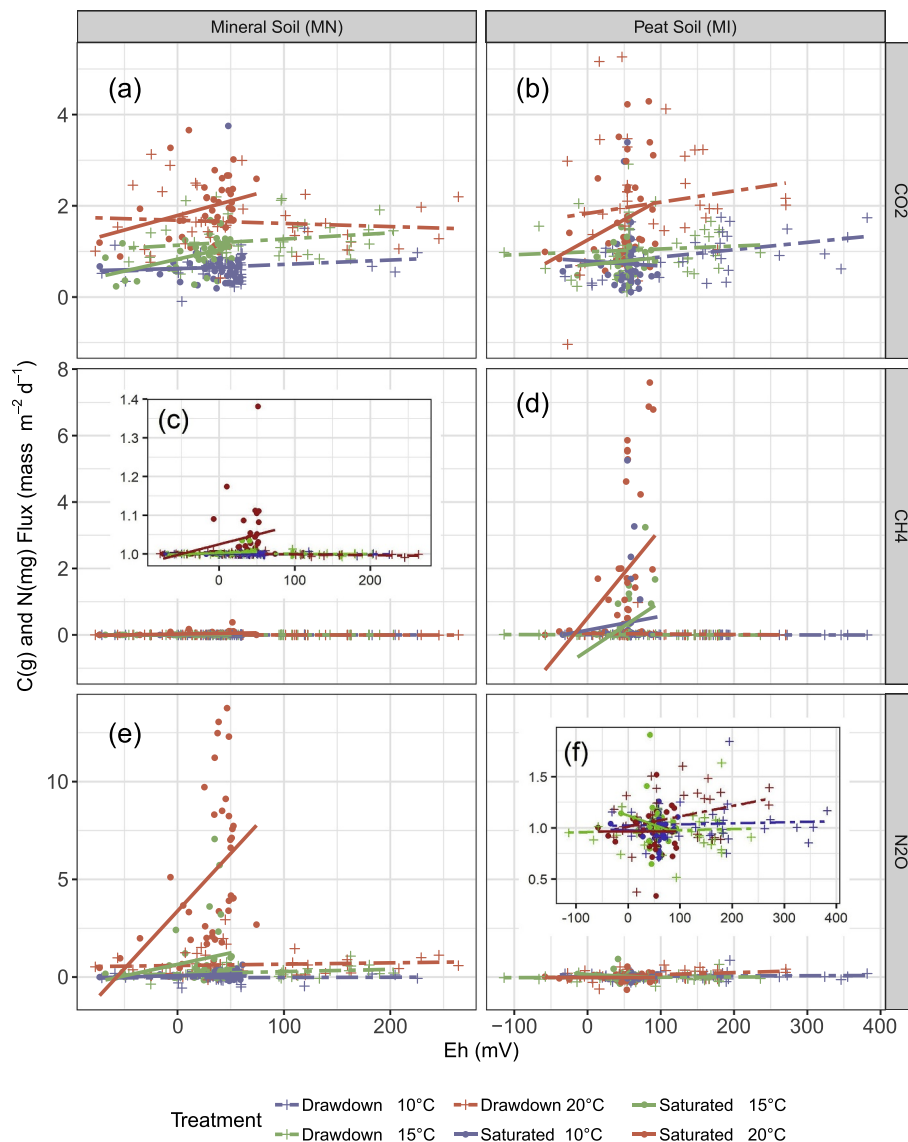


**Fig. 4.** Scatter plots of gas fluxes vs redox grouped by treatment with linear mean functions displayed as solid or dashed lines for the saturated or drawdown water-level treatments respectively. The  $\text{CH}_4$  mineral soil (c) and  $\text{N}_2\text{O}$  peat soil (f) panels include inset graphs with larger scales in addition to the small-scale graph.

#### 4.2. Methane

The saturated treatment in the peat soil from Upper Michigan had the greatest  $\text{CH}_4$  fluxes in the experiment, (Table 2). Each saturated treatment had greater cumulative fluxes than its drawdown counterpart indicating that water-level was the primary driver of  $\text{CH}_4$  fluxes in the peat soil. Additionally, the effect of water-level was amplified at greater temperatures, with the saturated-20 °C treatment having significant greater flux than all others (Table 2). The Eh data indicates that  $\text{CH}_4$  fluxes only occurred at  $\text{Eh} < 100$  mV and no  $\text{CH}_4$  is produced in the drawdown cores where mean Eh values are  $> 100$  mV. In contrast, all mineral soil treatments produced little-to-no  $\text{CH}_4$  ( $< 0.13$  g C  $\text{m}^{-2}$   $\text{day}^{-1}$ ) even though the saturated mineral soil had Eh values  $< 100$  mV. This could be associated with relatively low C substrate, as the mineral soil only had approximately 0.9% total soil C compared to  $> 50\%$  in the peat (Table 1). In support of this, there was a significant, albeit low ( $\sim 0.1$  g C  $\text{m}^{-2}$   $\text{day}^{-1}$ ), increase in  $\text{CH}_4$  fluxes in the saturated treatment at 20 °C in the mineral soil which could result under low C substrate availability. In addition, the mineral soil produced  $\text{N}_2\text{O}$  which indicates denitrifying bacteria were the dominant microbial population and the production of  $\text{CH}_4$  would not occur until

the  $\text{NO}_3^-$  in the soil was consumed (Vepraskas et al., 2016). Regardless the mechanism(s), our results indicate that mineral soil black ash wetlands are at minimal risk of increased  $\text{CH}_4$  fluxes following EAB disturbance. However, black ash wetlands with peat soils are likely to experience an increase in  $\text{CH}_4$  flux following EAB disturbance resulting in a loss of C from the ecosystem and transfer to the atmosphere.

In situ  $\text{CH}_4$  fluxes measured in Upper Michigan black ash wetlands with peat soil by Van Grinsven et al. (2018) were typically  $< 10$  mg C  $\text{m}^{-2}$   $\text{day}^{-1}$ , which is orders of magnitude less than the approximately 1 g C  $\text{m}^{-2}$   $\text{day}^{-1}$  measured in the 15 °C incubation chamber in this experiment. This large difference is likely caused by two factors. First, our experiment incubated soil cores containing approximately 45 cm of the soil column, in a setting where the entire soil column was the same temperature. Under field conditions, soil temperature would decrease with depth in the upper 45 cm of the soil column. The uniform temperature likely increased the microbial activity in the deeper soil above natural levels producing more  $\text{CH}_4$ . Secondly, ebullition events, a phenomenon in which trapped bubbles of methane are released from the soil, may have been increased in the soil cores. Van Grinsven et al. (2018) removed all  $\text{CH}_4$  flux samples with non-linear slopes (approximately 8% of  $\text{CH}_4$  data) from the analysis because they were thought to

be ebullition events and may have resulted from human disturbance during sampling. However, ebullition is a natural occurrence in wetlands, especially peatlands, and is an important mechanism by which  $\text{CH}_4$  is released to the atmosphere with fluxes reported in natural settings (Baird et al., 2004; Green and Baird, 2012; Kellner et al., 2006; Kettridge et al., 2011; Tokida et al., 2005). Ebullition events, controlled primarily by soil temperature and water level, were shown to account for > 38% of  $\text{CH}_4$  fluxes in temperate lowland floodplain fens (Stanley et al., 2019). Given this, we opted to include non-linear  $\text{CH}_4$  fluxes in our analysis which comprised 13% of our data in the peat soil (25% of the saturated treatments) to account for potential ebullition effects. Chen et al. (2019) also did not remove non-linear  $\text{CH}_4$  fluxes and calculated fluxes based on the initial slope of a non-linear concentration versus time relationship, but reported net consumption of  $\text{CH}_4$  in grassland soil cores and a small, fluctuating response in wetland soils. Doroski et al. (2019) excluded fluxes with weak linear relationships and reported  $\text{CH}_4$  fluxes about half the magnitude of ours in saturated coastal wetland soils. While disturbance to the soil cores during measurement was minimal, it could have increased ebullition events and edge flow during sampling, causing an over estimation of  $\text{CH}_4$  fluxes from these wetland soils under the conditions of the incubation. Because of the above, our estimates are likely not directly comparable to fluxes in a natural setting. However, the high occurrence of non-linear fluxes at warm temperatures indicate potentially critical importance of ebullition events to  $\text{CH}_4$  fluxes in this system, but more research is required to quantify ebullition contributions especially in field settings. Regardless, our results indicate that increased temperature in saturated peat soil will result in increased  $\text{CH}_4$  fluxes.

#### 4.3. Nitrous oxide

In contrast to  $\text{CH}_4$ , the most significant treatment effects for  $\text{N}_2\text{O}$  occurred in the mineral soil from northern Minnesota. The observed  $\text{N}_2\text{O}$  fluxes were similar in magnitude to fluxes in incubated mineral soil cores from calcareous wetlands in northern Minnesota (Berryman et al., 2009), riparian wetlands in temperate, continental China (Chen et al., 2019), and slightly greater than intact soil cores from coastal wetlands in the United States (Doroski et al., 2019). In the mineral soil, the saturated treatment at 20 °C produced significantly more  $\text{N}_2\text{O}$  than the other treatments. In contrast,  $\text{N}_2\text{O}$  flux was very low ( $< 0.28 \text{ mg m}^{-2} \text{ day}^{-1}$ ) from the peat soil regardless of treatment (Fig. 2f). Of the observed  $\text{N}_2\text{O}$  fluxes  $> 1 \text{ mg N m}^{-2} \text{ day}^{-1}$  ( $n = 52$ ), 87% of them fell in the Eh range 0 to 55 mV and few occurred at Eh  $< 0 \text{ mV}$  ( $n = 3$ ) or  $> 55 \text{ mV}$  ( $n = 4$ ).

Based on the post-experiment soil chemistry data (Table 1), the peat soil had total N (~2.4%) that is an order of magnitude greater than the mineral soil (~0.1%). Total soil N in the peat soil is distributed relatively evenly by depth, but in the mineral soil most of the N is in the upper 15 cm of the soil column (Toczydlowski, 2018). We think it is likely that the depth distribution of soil N relative to the water-level is the primary driver of the  $\text{N}_2\text{O}$  response in the mineral cores. Since denitrification is an anaerobic process, there was little opportunity for  $\text{NO}_3^-$  to be denitrified in the upper 15 cm of the drawdown treatment, resulting in little  $\text{N}_2\text{O}$  production. Maintaining a water table below about 15 cm depth in black ash wetlands may avoid large  $\text{N}_2\text{O}$  fluxes. While the peat soil has approximately 2.4% total N, the sustained saturation in natural settings greatly slows decomposition so that most of the N likely remains in organic forms and is not available for denitrification even if there are suitable anaerobic conditions. A more prolonged drawdown period may be required to mineralize organic N in the peat soil. Based on porewater chemistry data (Toczydlowski, 2018), at the end of the experiment the saturated treatment had similar and low (~0.1  $\text{mg L}^{-1}$ ) total  $\text{NO}_2^-$  plus  $\text{NO}_3^-$  concentrations for both mineral and peat soils, but the peat porewater had greater  $\text{NH}_4^+$  and total N than the mineral soil porewater. Both soil types had greater total N than inorganic N indicating much of the N in the porewater is in

organic forms. Ammonification can occur at low rates in anaerobic soils allowing  $\text{NH}_4^+$  to accumulate in the saturated peat, but in the absence of oxidized rhizospheres, there is little opportunity for the aerobic conversion of  $\text{NH}_4^+$  to  $\text{NO}_2^-$  or  $\text{NO}_3^-$ , accounting for the imbalance of  $\text{NH}_4^+$  and  $\text{NO}_2^-$  and  $\text{NO}_3^-$  in the peat porewater and the lack of  $\text{N}_2\text{O}$  production in the peat soil.

Our results show that black ash wetlands with peat soils will likely not experience changes in  $\text{N}_2\text{O}$  fluxes, but black ash wetlands with mineral soils, like those in northern Minnesota, will experience an increase in  $\text{N}_2\text{O}$  fluxes following EAB disturbance resulting in both a loss of important, limiting nutrients from the ecosystem, and an increased flux of a powerful greenhouse gas to the atmosphere.

#### 4.4. Temperature

The effect of temperature on gas fluxes is apparent for all gas species (Fig. 2), with gas fluxes increasing with increasing temperature and generally becoming more variable as indicated by the standard error. In  $\text{N}_2\text{O}$  and  $\text{CH}_4$  fluxes, water-level treatment effects were more pronounced at warmer temperatures, where they were minimal or non-existent at low temperatures. These trends have been observed in numerous in-situ and laboratory studies (Kellner et al., 2006; Maag and Vinther, 1996; Phillips et al., 2014; Van Grinsven et al., 2018). For context, mean July soil temperatures at 10 cm depth were 15.0 °C and 15.9 °C in the Upper Michigan and northern Minnesota sites with maximum daily temperatures reaching 18 °C to 20 °C. An EAB invasion in the current climate may result in changes like those observed in the 15 °C treatments in this experiment, but the uniform temperature of the soil cores likely overestimated absolute flux values compared to natural settings where soil temperature decreases with depth. Realistically, much warmer temperatures in the field would likely be required to produce  $\text{N}_2\text{O}$  and  $\text{CH}_4$  fluxes of a similar magnitude to this experiment. Still, EAB disturbance that leads to warmer soil temperatures will likely increase the rates of  $\text{CO}_2$ ,  $\text{N}_2\text{O}$ , and  $\text{CH}_4$  fluxes from black ash wetlands soils.

#### 4.5. Inference and limitations

Studying intact soil cores in a laboratory incubation has value because independent variables like temperature, humidity, and soil moisture can be controlled. However, artifacts of using soil cores limit the ability to make direct comparisons to conditions in natural ecosystems. In the incubation, soil cores are at a uniform temperature at all depths, lack vegetation, and do not have the same water movement as in the field. These factors, in addition to possible edge flow of gases along the PVC core, likely result in absolute gas fluxes greater than would be measured in situ. The incubation experiment is designed for making relative comparisons among treatments and using the results to make inferences about relative changes in fluxes in natural ecosystems. Inferences regarding Eh are also limited because Eh is notably variable over time and the Eh and gas flux measurements were taken up to 24 h apart.

#### 4.6. Conclusion

Watershed-scale ash mortality caused by EAB in black ash wetlands is predicted to cause a cascade of ecosystem changes including changes in carbon and nutrient cycling. The results of this soil core incubation experiment indicate differential responses of gas fluxes to water levels and soil temperature in northern Minnesota and Upper Michigan black ash wetland soils. Site location, and therefore soil type, was an important factor for  $\text{N}_2\text{O}$  and  $\text{CH}_4$  fluxes, where higher  $\text{N}_2\text{O}$  fluxes occurred in the mineral soils from northern Minnesota, and the only substantial  $\text{CH}_4$  fluxes came from the peat soil from Upper Michigan. Within a site, water-level had notable effects on  $\text{N}_2\text{O}$  and  $\text{CH}_4$  fluxes, with saturated cores having the greatest fluxes. Based on this analysis,

there were minimal significant treatment effects in CO<sub>2</sub> fluxes and the values were similar between soil types and water-level treatments. Temperature effects on gas fluxes were apparent in that fluxes of all gas species increased and had greater variation as temperature increased. Water-level treatment effects were also more pronounced at higher temperatures.

Based on the results of this laboratory experiment, it is likely that cascading effects of emerald ash borer invasion will lead to increased fluxes of N<sub>2</sub>O and CH<sub>4</sub>, both powerful greenhouse gasses. Future field experiments studying nutrient dynamics in these wetland soils will be needed to quantify the impacts of EAB on ecosystem functions under natural conditions. This study highlights the importance of mitigating EAB impacts to avoid increased greenhouse emissions and loss of nutrients from the soil in black ash wetlands.

## Acknowledgements

This research was funded in part by the Minnesota Forest Resources Council, USDA Forest Service Northern Research Station, and the University of Minnesota Department of Forest Resources. We gratefully acknowledge Anne Gapinski, Joseph Shannon, Mitchell Slater, and David and Patricia Toczydlowski for assistance with fieldwork, and Nathan Aspelin, Douglas Brinkman, Cindy Buschena, Michael Dolan, and the USDA USFS Northern Research Station for conducting and assisting with laboratory analyses.

## Declaration of competing interest

The authors declare that they have no known competing financial interests or personal relationships that could have appeared to influence the work reported in this paper.

## References

- Altshuler, I., Hamel, J., Turney, S., Magnuson, E., Lévesque, R., Greer, C.W., Whyte, L.G., 2019. Species interactions and distinct microbial communities in high Arctic permafrost affected cryosols are associated with the CH<sub>4</sub> and CO<sub>2</sub> gas fluxes. *Environ. Microbiol.* 21 (10), 3711–3727. <https://doi.org/10.1111/1462-2920.14715>.
- Baird, A.J., Beckwith, C.W., Waldron, S., Waddington, J.M., 2004. Ebullition of methane-containing gas bubbles from near-surface Sphagnum peat. *Geophys. Res. Lett.* 31, 2–5. <https://doi.org/10.1029/2004GL021157>.
- Berryman, E.M., Venterea, R.T., Baker, J.M., Bloom, P.R., Elf, B., 2009. Phosphorus and greenhouse gas dynamics in a drained calcareous wetland soil in Minnesota. *J. Environ. Qual.* 38, 2147–2158. <https://doi.org/10.2134/jeq2008.0409>.
- Chen, Y., Whitehill, J.G.A., Bonello, P., Poland, T.M., 2011. Feeding by emerald ash borer larvae induces systemic changes in black ash foliar chemistry. *Phytochemistry* 72, 1990–1998. <https://doi.org/10.1016/j.phytochem.2011.07.003>.
- Chen, W., Zheng, X., Wolf, B., Yao, Z., Liu, C., Butterbach-Bahl, K., Brüggemann, N., 2019. Long-term grazing effects on soil-atmosphere exchanges of CO<sub>2</sub>, CH<sub>4</sub> and N<sub>2</sub>O at different grasslands in Inner Mongolia: a soil core study. *Ecol. Indic.* 105, 316–328. <https://doi.org/10.1016/j.ecolind.2017.09.035>.
- Davis, J.C., Shannon, J.P., Bolton, N.W., Kolka, R.K., Pypker, T.G., 2017. Vegetation responses to simulated emerald ash borer infestation in *Fraxinus nigra* dominated wetlands of Upper Michigan, USA. *Can. J. For. Res.* 47, 319–330. <https://doi.org/10.1139/cjfr-2016-0105>.
- De Klein, C.A.M., Harvey, M., 2012. Nitrous Oxide Chamber Methodology Guidelines. Global Research Alliance on Agricultural Greenhouse Gases.
- de Mendiburu, F., 2017. *agricolae: Statistical Procedures for Agricultural Research*.
- DeBusk, W.F., Reddy, K.R., 2003. Nutrient and hydrology effects on soil respiration in a Northern Everglades marsh. *J. Environ. Qual.* 32, 702–710. <https://doi.org/10.2134/jeq2003.7020>.
- Diamond, J.S., McLaughlin, D., Slesak, R.A., D'Amato, A.W., Palik, B.J., 2018. Forested versus herbaceous wetlands: can management mitigate ecophysiological regime shifts from invasive emerald ash borer? *J. Environ. Manag.* 222, 436–446. <https://doi.org/10.1016/j.jenvman.2018.05.082>.
- Doroski, A.A., Helton, A.M., Vadas, T.M., 2019. Greenhouse gas fluxes from coastal wetlands at the intersection of urban pollution and saltwater intrusion: a soil core experiment. *Soil Biol. Biochem.* 131, 44–53. <https://doi.org/10.1016/j.soilbio.2018.12.023>.
- Ebrahimi, A., Or, D., 2016. Microbial community dynamics in soil aggregates shape biogeochemical gas fluxes from soil profiles - upscaling an aggregate biophysical model. *Glob. Change Biol.* 22 (9), 3141–3156. <https://doi.org/10.1111/gcb.13345>.
- Fiedler, S., Vepraskas, M.J., Richardson, J.L., 2007. Soil redox potential: importance, field measurements, and observations. In: *Adv. Agron. Elsevier Masson SAS*. [https://doi.org/10.1016/S0065-2113\(06\)94001-2](https://doi.org/10.1016/S0065-2113(06)94001-2).
- Fox, J., Weisberg, S., 2011. *An {R} Companion to Applied Regression*.
- Green, S.M., Baird, A.J., 2012. A mesocosm study of the role of the sedge *Eriophorum angustifolium* in the efflux of methane-including that due to episodic ebullition from peatlands. *Plant Soil* 351, 207–218. <https://doi.org/10.1007/s11104-011-0945-1>.
- Hammer, P.A., Hopper, D.A., 1997. *Experimental design*. In: *Growth Chamber Handbook*, pp. 177–188.
- Hermes, D.A., McCullough, D.G., 2014. Emerald ash borer invasion of North America: history, biology, ecology, impacts, and management. *Annu. Rev. Entomol.* 59, 13–30. <https://doi.org/10.1146/annurev-ento-011613-162051>.
- Hinchey, E.K., Schaffner, L.C., 2005. An evaluation of electrode insertion techniques for measurement of redox potential in estuarine sediments. *Chemosphere* 59, 703–710. <https://doi.org/10.1016/j.chemosphere.2004.10.029>.
- Hou, A.X., Chen, G.X., Wang, Z.P., Van Cleemput, O., Patrick, W.H., 2000. Methane and nitrous oxide emissions from a rice field in relation to soil redox and microbiological processes. *Soil Sci. Soc. Am. J.* 64, 2180. <https://doi.org/10.2136/sssaj2000.6462180x>.
- Kahlert, H., 2010. Reference electrodes. In: *Electroanalytical Methods*. Springer Berlin Heidelberg, Berlin, Heidelberg, pp. 291–308. [https://doi.org/10.1007/978-3-642-02915-8\\_15](https://doi.org/10.1007/978-3-642-02915-8_15).
- Kellner, E., Baird, A.J., Oosterwoud, M., Harrison, K., Waddington, J.M., 2006. Effect temperature and atmospheric pressure on methane (CH<sub>4</sub>) ebullition from near-surface peats. *Geophys. Res. Lett.* 33, 1–5. <https://doi.org/10.1029/2006GL027509>.
- Kettridge, N., Binley, A., Green, S.M., Baird, A.J., 2011. Ebullition events monitored from northern peatlands using electrical imaging. *J. Geophys. Res. Biogeosci.* 116, 1–14. <https://doi.org/10.1029/2010JG001561>.
- Knight, K.S., Brown, J.P., Long, R.P., 2013. Factors affecting the survival of ash (*Fraxinus* spp.) trees infested by emerald ash borer (*Agrius planipennis*). *Biol. Invasions* 15, 371–383. <https://doi.org/10.1007/s10530-012-0292-z>.
- Kolka, R.K., D'Amato, A.W., Wagenbrenner, J.W., Slesak, R.A., Pypker, T.G., Youngquist, M.B., Grinde, A.R., Palik, B.J., 2018. Review of ecosystem level impacts of emerald ash borer on black ash wetlands: what does the future hold? *Forests* 9, 1–15. <https://doi.org/10.3390/f9040179>.
- Lenth, R.V., 2016. Least-squares Means: The R Package lsmeans. <https://doi.org/10.18637/jss.v069.i01>.
- Light, T.S., 1972. Standard solution for redox potential measurements. *Anal. Chem.* 44, 1038–1039. <https://doi.org/10.1021/ac60314a021>.
- Looney, C.E., D'Amato, A.W., Palik, B.J., Slesak, R.A., 2015. Overstory treatment and planting season affect survival of replacement tree species in emerald ash borer threatened *Fraxinus nigra* forests in Minnesota, USA. *Can. J. For. Res.* 45, 1728–1738. <https://doi.org/10.1139/cjfr-2015-0129>.
- Maag, M., Vinther, F.P., 1996. Nitrous oxide emission by nitrification and denitrification in different soil types and at different soil moisture contents and temperatures. *Appl. Soil Ecol.* 4, 5–14. [https://doi.org/10.1016/0929-1393\(96\)00106-0](https://doi.org/10.1016/0929-1393(96)00106-0).
- MacFarlane, D.W., Meyer, S.P., 2005. Characteristics and distribution of potential ash tree hosts for emerald ash borer. *Forest Ecol. Manag.* 213, 15–24. <https://doi.org/10.1016/j.foreco.2005.03.013>.
- Nisbet, D., Kreuzweiser, D., Sibley, P., Scarr, T., 2015. Ecological risks posed by emerald ash borer to riparian forest habitats: a review and problem formulation with management implications. *Forest Ecol. Manag.* 358, 165–173. <https://doi.org/10.1016/j.foreco.2015.08.030>.
- Palik, B.J., Ostry, M.E., Venette, R.C., Abdela, E., 2011. *Fraxinus nigra* (black ash) dieback in Minnesota: regional variation and potential contributing factors. *Forest Ecol. Manag.* 261, 128–135. <https://doi.org/10.1016/j.foreco.2010.09.041>.
- Palik, B.J., Ostry, M.E., Venette, R.C., Abdela, E., 2012. Tree regeneration in black ash (*Fraxinus nigra*) stands exhibiting crown dieback in Minnesota. *Forest Ecol. Manag.* 269, 26–30. <https://doi.org/10.1016/j.foreco.2011.12.020>.
- Perry, K.I., Hermes, D.A., 2016. Response of the forest floor invertebrate community to canopy gap formation caused by early stages of emerald ash borer-induced ash mortality. *Forest Ecol. Manag.* 375, 259–267. <https://doi.org/10.1016/j.foreco.2016.05.034>.
- Phillips, R.L., McMillan, A.M.S., Palmada, T., Dando, J., Giltrap, D., 2014. Temperature effects on N<sub>2</sub>O and N<sub>2</sub> denitrification end-products for a New Zealand pasture soil. *New Zeal. J. Agr. Res.* 58, 89–95. <https://doi.org/10.1080/00288233.2014.969380>.
- Pinheiro, J., Bates, D., Debroy, S., Sarkar, D., R Core Team, 2017. *nlme: Linear and Nonlinear Mixed Effects Models*.
- R Core Team, 2017. *R: A Language and Environment for Statistical Computing*.
- Scholz, F., 2010. *Electroanalytical Methods - Electrolytes*. <https://doi.org/10.1007/978-3-642-02915-8>.
- Slesak, R.A., Lenhart, C.F., Brooks, K.N., D, A.W., Palik, B.J., Slesak, R., Brooks, K., Palik, B., 2014. Water table response to harvesting and simulated emerald ash borer mortality in black ash wetlands in Minnesota, USA. *Can. J. For. Res. Can. J. For. Res.* 44, 961–96817. <https://doi.org/10.1139/cjfr-2014-0111>.
- Smith, K.A., Ball, T., Conen, F., Dobbie, K.E., Massheder, J., Rey, A., 2003. Exchange of greenhouse gases between soil and atmosphere: interactions of soil physical factors and biological processes. *Eur. J. Soil Sci.* 69, 10–20. <https://doi.org/10.1111/ejss.12539>.
- Smitley, D., Davis, T., Rebek, E., 2008. Progression of ash canopy thinning and dieback outward from the initial infestation of emerald ash borer (Coleoptera: Buprestidae) in

- southeastern Michigan. *J. Econ. Entomol.* 101, 1643–1650. [https://doi.org/10.1603/0022-0493\(2008\)101\[1643:POACTA\]2.0.CO;2](https://doi.org/10.1603/0022-0493(2008)101[1643:POACTA]2.0.CO;2).
- Stanley, K.M., Heppell, C.M., Belyea, L.R., Baird, A.J., Field, R.H., 2019. The importance of CH<sub>4</sub> ebullition in floodplain fens. *J. Geophys. Res.-Biogeo.* 124, 1750–1763. <https://doi.org/10.1029/2018JG004902>.
- Telander, A.C., Slesak, R.A., D'Amato, A.W., Palik, B.J., Brooks, K.N., Lenhart, C.F., 2015. Sap flow of black ash in wetland forests of northern Minnesota, USA: hydrologic implications of tree mortality due to emerald ash borer. *Agric. For. Meteorol.* 206, 4–11. <https://doi.org/10.1016/j.agrformet.2015.02.019>.
- Toczydlowski, A.J., 2018. Effects of Simulated Emerald Ash Borer Disturbance on Carbon and Nitrogen Cycling in Black Ash Wetland Soils in the Great Lakes Region. University of Minnesota, USA.
- Tokida, T., Miyazaki, T., Mizoguchi, M., 2005. Ebullition of methane from peat with falling atmospheric pressure. *Geophys. Res. Lett.* 32, 1–4. <https://doi.org/10.1029/2005GL022949>.
- Van Grinsven, M.J., Shannon, J.P., Davis, J.C., Bolton, N.W., Wagenbrenner, J.W., Kolka, R.K., Pypker, T.G., 2017. Source water contributions and hydrologic responses to simulated emerald ash borer infestations in depressional black ash wetlands. *Ecohydrology* 10, 1–13. <https://doi.org/10.1002/eco.1862>.
- Van Grinsven, M.J., Shannon, J., Bolton, N., Davis, J., Noh, N., Wagenbrenner, J., Kolka, R., Pypker, T., 2018. Response of black ash wetland gaseous soil carbon fluxes to a simulated emerald ash borer infestation. *Forests* 9, 324. <https://doi.org/10.3390/f9060324>.
- Vepraskas, M.J., Polizzotto, M., Faulkner, S.P., 2016. Redox chemistry of hydric soils. In: Vepraskas, M.J., Craft, C.B. (Eds.), *Wetland Soils: Genesis, Hydrology, Landscapes, and Classification*. CRC Press, Boca Raton, FL, pp. 105–132.
- Wang, Z.P., DeLaune, R.D., Masscheleyn, P.H., Patrick, W.H., 1993. Soil redox and pH effects on methane production in a flooded rice soil. *Soil Sci. Soc. Am. J.* 57, 382. <https://doi.org/10.2136/sssaj1993.03615995005700020016x>.
- Yang, J., Liu, J., Hu, X., Li, X., Wang, Y., Li, H., 2013. Effect of water table level on CO<sub>2</sub>, CH<sub>4</sub> and N<sub>2</sub>O emissions in a freshwater marsh of Northeast China. *Soil Biol. Biochem.* 61, 52–60. <https://doi.org/10.1016/j.soilbio.2013.02.009>.
- Youngquist, M.B., Eggert, S.L., D'Amato, A.W., Palik, B.J., Slesak, R.A., 2017. Potential effects of foundation species loss on wetland communities: a case study of black ash wetlands threatened by emerald ash borer. *Wetlands* 37, 787–799. <https://doi.org/10.1007/s13157-017-0908-2>.